Simulation of Meshing for the Spur Gear Drive with Modified Tooth Surfaces

Inhwan Seol*, Soonbae Chung
Senior Researcher Agency for Defence Development

The authors have proposed methods (lead crowning and profile modification) for modifying the geometry of spur gears and investigated the contact pattern as well as the transmission errors to recommend the appropriate amount of modification. Based on the investigation, dynamic load of the modified spur gear drive has been calculated, which is helpful to predict the life of the designed gear drive. Computer programs for simulation of meshing, contact and dynamics of the modified spur gears have been developed. The developed theory is illustrated with numerical examples.

Key Words : Spur Gear, Crowning, Transmission Error

1. Introduction

Involute spur gears have been widely applied in industry because of low cost of manufacturing. Ideal spur gears with line contact are very sensitive to misalignment and manufacturing errors which cause the edges of the gear drive to contact.

The easiest way to avoid the edge contact is to localize the bearing contact by crowning the gear tooth surfaces (Townsend, 1991). This means that the line contact of surfaces is changed to point contact. In addition, modification of the tooth profile is required. An increased magnitude of crowning weakens the pitting durability, and insufficient crowning decreases the ability to stabilize the bearing contact. Although crowning is a very important manufacturing technique in gears sufficient analysis for the proper amount of crowning has not been provided.

The most common way of crowning is the so called lead crowning. In this paper, lead crowning is modeled as the deviation of surface of revolution from the theoretical surface (Fig. 1 (a)). The generating curve of the surface of revolution is an exact involute one. After modeling the crowning characteristics, TCA (Tooth Contact Analysis) is performed in order to investigate the crowning effect on the stabilization and the size of bearing contact as well as the induced transmission errors.

The next step is to determine the dynamic effect of the transmission errors in contact force of the gear drive. The determination of the dynamic force plays a key role in predicting the life of the designed gear drive (Savage, et al., 1988). Precise prediction can improve the reliability of the gear design. The dynamic load on a gear teeth has been previously investigated experimentally and theoretically. However, there has not been an attempt to study the dynamics of gears related to the transmission errors caused by misalignment and manufacturing errors. The dynamics of gearing is a very complex problem because it is basically a nonlinear and time-varying problem (Kahraman and Blankenship, 1997; Lin, et al., 1988; Matsumura, et al., 1996; Wang, 1985). This paper is an attempt toward more exact analysis of gearing.

* Corresponding Author,
E-mail : seolkoo@chollian.net
TEL : +82-42-863-8553
Senior Researcher, Agency for Defence Development, P.O. Box 35-1, Yusong, Taejon 305-600, Korea.
(Manuscript **Received** June 9, 1999; **Revised** February 21, 2000)

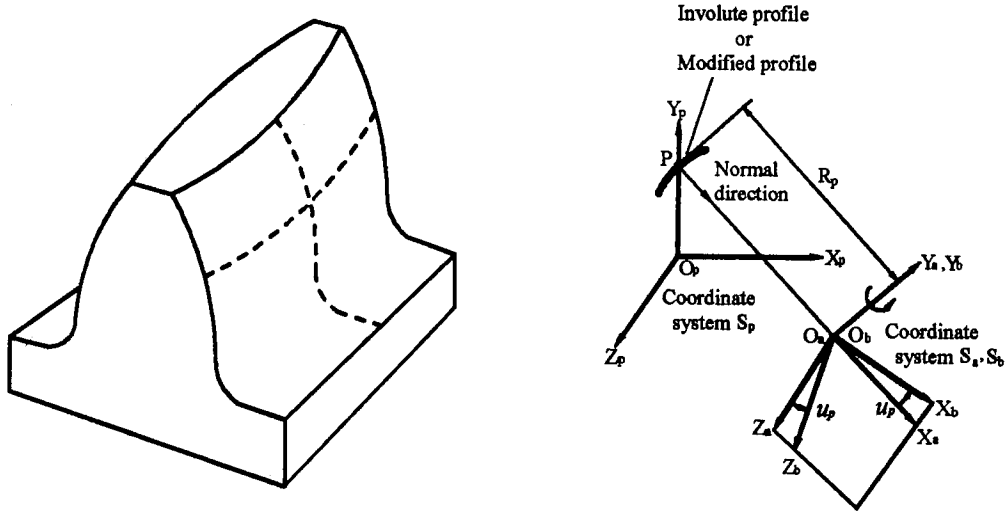

(a) (b)

Fig. 1 (a) Modified Tooth Surface of the spur gear
(b) Coordinate systems for generation of modified tooth surfaces

2. Modeling of the Crowned Spur Gear Surface

The lead crowning of a spur gear can be considered as the longitudinal deviation from a straight line along the tooth face width(1976). The authors consider that the tooth profile in the cross section including the pitch point P is an involute curve. The deviation by crowning can be obtained in various ways. The tooth surfaces are represented as the surface of revolution that is generated by rotation of the involute curve about a fixed axis.

Figure 1(b) shows the generation procedure of a crowned pinion tooth surface. Coordinate system S_p is used for describing the pinion surface. First, the involute profile is represented in $X_p - Y_p$ plane in parametric representation of a space curve

$$\mathbf{r}_p = \mathbf{r}_p(\theta_p) \tag{1}$$

Here, $\mathbf{r}_p$ is the vector which represents involute curve and θ_p is the variable parameter.

In the auxiliary coordinate system S_a, Y_a and X_a axes coincide with the tangential vector and normal vector at pitch point P, respectively. The origin O_a is positioned at a distance R_p from P measured along the direction of the normal. R_p is the radius of revolution and it controls the amount of crowning. The surface of revolution is generated in another auxiliary coordinate system S_b by rotating the involute profile about the Y_a axis. Finally, after the coordinate transformation, the crowned pinion tooth surface $\sum_p$ is represented as follows:

$$\mathbf{r}_p(\theta_p, u_p, R_p) = \mathbf{M}_{pb}\mathbf{M}_{ba}\mathbf{M}_{ap}\mathbf{r}_p(\theta_p) \tag{2}$$

Here, u_p is the angle of revolution and $\mathbf{M}$ is a coordinate transformation matrix. If R_p is given, the pinion tooth surface is represented in two-parameter form where parameters θ_p and u_p are independent.

Similar procedure can be applied for generation of gear tooth surface. The crowned gear tooth surface $\sum_g$ is obtained as

$$\mathbf{r}_g = \mathbf{r}_g(\theta_g, u_g, R_g) \tag{3}$$

3. Tooth Contact Analysis of the Crowned Spur Gear Drive

3.1 Basic principles of simulation of meshing and contact (Litvin, 1989)

Two cases of simulation of meshing and contact are considered, which cover point contact and line contact of surfaces.

Case 1. The contact of interacting surfaces $\sum_p$ and $\sum_g$ is localized and they are in point tangen-

cy. The tooth surfaces and their unit normals are represented in a common fixed coordinate system S_f. The conditions of continuous tangency of the meshing surfaces are represented by the equations

$$\mathbf{r}_f^{(p)}(u_p, \theta_p, \phi_p) - \mathbf{r}_f^{(g)}(u_g, \theta_g, \phi_g) = 0 \quad (4)$$

$$\mathbf{n}_f^{(p)}(u_p, \theta_p, \phi_p) - \mathbf{n}_f^{(g)}(u_g, \theta_g, \phi_g) = 0 \quad (5)$$

Here, (u_i, θ_i), $(i=p, g)$ are the surface parameters, ϕ_i is the angle of rotation, $\mathbf{r}_f^{(i)}$ is the position vector of surface $\sum_i$, and $\mathbf{n}_f^{(i)}$ is the surface unit normal $(i=p, g)$. Equations (4) and (5) yield only five independent scalar equations since $|\mathbf{n}_f^{(p)}| = |\mathbf{n}_f^{(g)}| = 1$. Thus, we have a system of five nonlinear equations and six unknowns:

$$f_i(u_p, \theta_p, \phi_p, u_g, \theta_g, \phi_g) = 0,$$
$$f_i \in C^1 \ (i=1, 2, \cdots, 5) \quad (6)$$

Considering one unknown, say ϕ_p, as the input, we can solve Eq. (6) by functions $u_p(\phi_p)$, $\theta_p(\phi_p)$, $u_g(\phi_p)$, $\theta_g(\phi_p)$, $\phi_g(\phi_p)$. The numerical computation is a continuous iterative process that requires an initial guess and the observation of the following inequality for each iteration.

$$\Delta_5 = \frac{D(f_1, f_2, f_3, f_4, f_5)}{D(u_p, \theta_p, u_g, \theta_g, \phi_g)} = \begin{vmatrix} \frac{\partial f_1}{\partial u_p} & \frac{\partial f_1}{\partial \theta_p} & \frac{\partial f_1}{\partial u_g} & \frac{\partial f_1}{\partial \theta_g} & \frac{\partial f_1}{\partial \phi_g} \\ \vdots & \vdots & \vdots & \vdots & \vdots \\ \frac{\partial f_5}{\partial u_p} & \frac{\partial f_5}{\partial \theta_p} & \frac{\partial f_5}{\partial u_g} & \frac{\partial f_5}{\partial \theta_g} & \frac{\partial f_5}{\partial \phi_g} \end{vmatrix} \neq 0 \quad (7)$$

Expressions

$$\mathbf{r}_i(u_i, \theta_i), \ u_i(\phi_p), \ \theta_i(\phi_p) \quad (i=1, 2) \quad (8)$$

represent the path of contact on gear tooth surface $\sum_i$. The function of transmission errors is represented as

$$\Delta\phi_g(\phi_p) = \phi_g(\phi_p) - \frac{N_p}{N_g}\phi_p \quad (9)$$

where N_p and N_g are the number of teeth in pinion and gear, respectively. Subroutine *DNEQNF* in *IMSL* Math Library is applied for the solution of nonlinear Eq. (6).

Case 2. The spur pinion and gear surfaces of ideal design are in line contact in the case of an aligned drive. The Jacobian Δ_5 in Eq. (7) becomes zero in this case. Due to misalignment, the line contact of surfaces results in point contact that is accompanied with the shift of the bearing contact and transmission errors. The simulation of meshing and contact of gear drives with a preliminary line contact is a complex problem since the Jacobian Δ_5 becomes equal to zero. The computational procedure that was developed in the previous study (Litvin, 1989; Seol and Litvin, 1996) overcomes these difficulties.

The authors have developed computer programs for the simulation of meshing and contact of conventional and modified spur-gear drives. The bearing contact is obtained as the set of instantaneous contact ellipses.

3.2 Simulation of meshing with errors of alignments and manufacture

The applied coordinate systems are shown in Fig. 2. Coordinate systems S_p and S_g are rigidly connected to the pinion and gear, and they are rotated about the Z_p and Z_g axes, respectively. Coordinate system S_f is the fixed one where the continuous tangency of $\sum_p$ and $\sum_g$ is considered. Coordinate system S_2 is an auxiliary fixed one, and coordinate system S_q is used for simulation of the misalignment.

Two types of misalignment will be considered; the change of center distance, ΔE and the change of shaft angle, γ_y. Two types of manufacturing error will be considered; the error of pressure angle, $\Delta\alpha$ and the variation of lead angle, $\Delta\lambda$.

The geometric defects mentioned above may affect the contact path and kinematic transmission errors, and consequently, the dynamic phenomena of gear drive. Therefore, the simulation of misaligned gear drive with manufacturing errors is a key point of this study.

3.3 Determination of contact ellipse

The determination of the instantaneous contact ellipse is a very important step especially to calculate the contact stress which is the key factor in pitting durability. It requires the knowledge of principal curvatures, directions of the spur pinion and gear tooth surfaces and the elastic approach of the teeth.

Assuming that two surfaces $\sum_1$ and $\sum_2$ are in point contact, we consider that the contact of surfaces is spread under the load over an elliptical

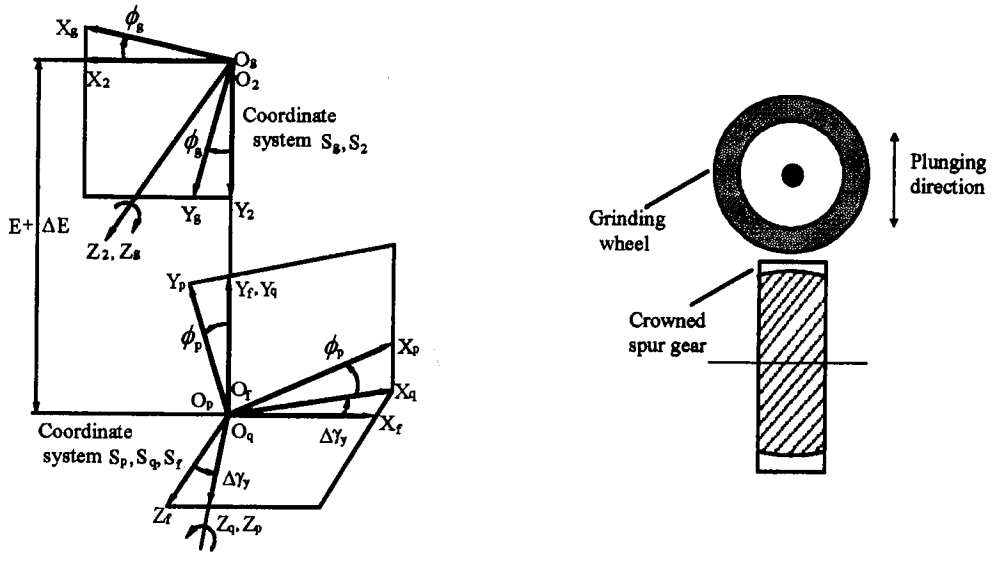

(a) (b)

Fig. 2 (a) Coordinate systems applied for simulation of meshing
(b) plunging operation for the parabolic transmission errors

area. The dimensions and orientations of the instantaneous contact ellipses can be determined when the following factors are known (Litvin, 1989; Seol and Litvin, 1996): (i) the principal directions and principal curvatures of interacting surfaces, and (ii) the elastic approach δ of surfaces. The surface approach δ can be determined if the contact forces applied to the surfaces and the surface curvatures are known. An approximate determination of the contact ellipse may be accomplished by using the δ value of 0.007 mm which is obtained from experiment for slightly loaded gear drives.

The determination of the orientation of the contact ellipse and its dimensions is based on the following procedure (Litvin, 1989):

Step 1 : It is considered that the principal directions and principal curvatures of the meshing surfaces are known, and the elastic approach of the surface is given.

Step 2 : The contacting surfaces $\sum_1$ and $\sum_2$ are in tangency at current point P, and $\prod$ is the plane that is tangent to $\sum_1$ and $\sum_2$ at P. Unit vectors $\mathbf{e}_I^{(i)}$ and $\mathbf{e}_{II}^{(i)}$ $(i=1, 2)$ represent the principal directions of surfaces $\sum_1$ and $\sum_2$, respectively. The orientation of the contact ellipse is represented by angle α that is determined as follows,

$$\tan 2\alpha = \frac{g_2 \sin 2\sigma^{(12)}}{g_1 - g_2 \cos 2\sigma^{(12)}} \tag{10}$$

where

$$g_1 = \varkappa_I^{(1)} - \varkappa_{II}^{(1)} \tag{11}$$

$$g_2 = \varkappa_I^{(2)} - \varkappa_{II}^{(2)} \tag{12}$$

Here, $\varkappa_I^{(i)}$ and $\varkappa_{II}^{(i)}$ are the principal curvatures of surface 1 and surface 2 at the contact point P, and $\sigma^{(12)}$ is the angle between $\mathbf{e}_I^{(1)}$ and $\mathbf{e}_I^{(2)}$.

Step 3 : The magnitudes of the ellipse semi-axes are determined by the equations

$$a = \left|\frac{\delta}{A}\right|^{\frac{1}{2}}, \quad b = \left|\frac{\delta}{B}\right|^{\frac{1}{2}} \tag{13}$$

where δ is the elastic approach; A and B are represented as

$$A = 0.25[\varkappa_\Sigma^{(1)} - \varkappa_\Sigma^{(2)} - (g_1^2 - 2g_1 g_2 \cos 2\sigma^{(12)} + g_2^2)^{\frac{1}{2}}] \tag{14}$$

$$B = 0.25[\varkappa_\Sigma^{(1)} - \varkappa_\Sigma^{(2)} - (g_1^2 - 2g_1 g_2 \cos 2\sigma^{(12)} + g_2^2)^{\frac{1}{2}}] \tag{15}$$

$$\varkappa_\Sigma^{(i)} = \varkappa_I^{(i)} + \varkappa_{II}^{(i)}, \quad i=1, 2 \tag{16}$$

The largest and smallest values of a and b represent the major and minor semi-axes of the contact ellipse, respectively.

4. Dynamic Analysis of Crowned Spur Gear Drive

It is well-known that the geometric errors of tooth surfaces affect thedynamics of gear drive. However, few attempts have been made to investigate the effect of geometric defect on the dynamic phenomena. In previous works(Lin, et al., 1988; Matsumura, et al., 1996; Lewicki, et al., 1993), the geometric defects, for example, tooth profile error, have been neglected or considered directly in terms of elastic force in dynamic equation (Fig. 3). In these models, the influence of geometric errors (misalignment and manufacturing errors) can not be investigated in full because the condition of contact of tooth surfaces is not considered.

The goal is to provide the analytical tool to investigate the influence of tooth geometry, manufacturing errors and misalignment on the dynamics of gear drive. To meet the goal, the authors investigate the dynamics of a gear drive with transmission errors as the dynamics of rigid bodies. The exact transmission errors induced by geometric defects have been determined by application of the TCA(Tooth Contact Analysis) approach.

Basic Assumptions:

To solve the dynamic equations of gear drive, following assumptions are made;

1. The contact of tooth surfaces is not discontinued.
2. There is no variation in input and output torques (steady torque).
3. Applied torque is light enough for meshed gears to be considered as rigid bodies.
4. Frictional force is neglected.

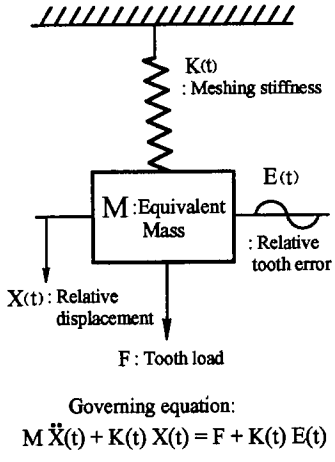

Fig. 3 Typical dynamic model of gear drive

4.1 Mathematical model and equations of motion

The mathematical model for a spur gear drive is shown in Fig. 4. This system is governed by the following equations of motion.

$$J_p \frac{d^2\phi_p}{dt^2} = T_{in} - T_d \tag{17}$$

$$J_g \frac{d^2\phi_g}{dt^2} = T_d - T_{out} \tag{18}$$

where gear ratio of the drive is considered as 1 : 1 ; J_p and J_g are mass moments of inertia of pinion and gear, respectively; ϕ_p and ϕ_g are angles of rotation of pinion and gear, respectively; T_{in} and T_{out} are the input and output (load) torque of gear drive, respectively; T_d is the dynamic torque to be determined.

The function of transmission error $\Delta\phi_g(\phi_p)$ can be represented as a function of ϕ_p and the time derivative as follows;

$$\Delta\phi_g(\phi_p) = \phi_g - \phi_p \tag{19}$$

$$\frac{d^2(\Delta\phi_g)}{dt^2} = \frac{d^2\phi_g}{dt^2} - \frac{d^2\phi_p}{dt^2} = \frac{d^2(\Delta\phi_g)}{d\phi_p^2}\left(\frac{d\phi_p}{dt}\right)^2 + \frac{d(\Delta\phi_g)}{d\phi_p}\frac{d^2\phi_p}{dt^2} \tag{20}$$

The transmission error function $\Delta\phi_g(\phi_p)$ can be determined by TCA. Since $\Delta\phi_g(\phi_p)$ is a periodic function with the period of the meshing cycle $\frac{2\pi}{N_p}$, it can be represented by the Fourier series as follows

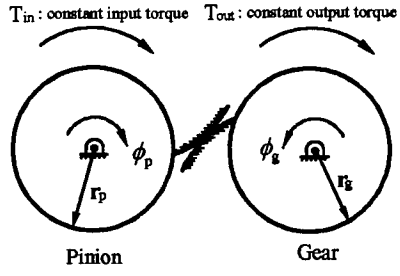

Fig. 4 Dynamic model of rigid body for gear drive

$$\Delta\phi_g(\phi_p)=A_0/2+A_1\cos N_p\phi_p+A_2\cos 2N_p\phi_p+A_3\cos 3N_p\phi_p+\cdots B_1\sin N_p\phi_p+B_2\sin 2N_p\phi_p+B_3\sin 3N_p\phi_p+\cdots \quad (21)$$

Here, A_i, $B_j(i=0, 1, 2, \cdots\ j=1, 2, \cdots)$ are the Fourier coefficients and can be determined by the results of TCA.

Now, if Eqs. (17), (18), (20) are solved with the initial conditions, the dynamic torque T_d can be determined. Afterward, to illustrate the dynamic effect clearly, we use *D. F.* (Dynamic Factor) as follows

$$D.F.=\frac{Dynamic\ Torque}{Static\ Torque} \quad (22)$$

The program for simulation of the dynamics of crowned spur gear has been developed by using the fourth order *Runge-Kutta* integration method.

5. Numerical Examples

The developed computer programs have been applied for the simulation of meshing and contact of crowned spur gear drives with geometric errors. The computations have been performed with the design parameters represented in Table 1.

The magnitude of crowning and the geometric errors are considered as follows;

Misalignment: change of center distance ΔE =0.1 mm; change of shaft angle $\Delta\gamma_y$=3.0 arc min;

Manufacturing errors: error of pressure angle $\Delta\alpha$=3.0 arc min; error of lead angle $\Delta\lambda$=3.0 arc min.

Table 1 Design parameters of spur pinion and gear

Number of pinion teeth	N_p=36
Number of gear teeth	N_g=36
Normal module	m_n=3.175 mm
Normal pressure angle	α_n=20°
Face width	FW=25.4 mm
Moment of inertia for pinion	$J_p=3.33\times10^{-3}$Kg m^2
Moment of inertia for gear	$J_g=3.33\times10^{-3}$Kg m^2

Modification: Case 1; 0.02 mm of lead crowning of both of pinion and gear, Case 2; 0.02 mm of lead crowning of pinion only, Case 3; 0.03 mm of lead crowning of both of pinion and gear, Case 4; 0.03 mm of lead crowning of both of pinion and gear and profile modification of pinion.

Figures 5, 6 and 7 show the bearing contact obtained for the considered gear drive with existing and modified geometries. The great advantage of the involute gear drive is the fact that the transmission errors caused by misalignment are small enough and may be ignored. On the other hand, errors of alignment cause a substantial shift in the bearing contact and the transmission errors induced by manufacturing errors can not be neglected (Fig. 5).

For dynamic simulation, the gear drive with the above mentioned geometric defect and Case 1 of lead crowning is selected. The driving torque is 160 Nm and the operating velocities are 900,

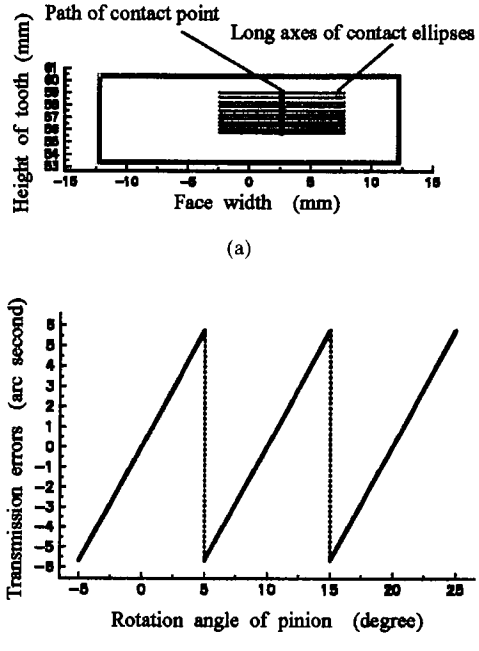

Fig. 5 (a) Bearing contact on pinion tooth surface (b) Corresponding transmission errors with lead crowning 0.02 mm of pinion; 0.02 mm of gear: misalignment; ΔE=0.1mm; $\Delta\gamma_y$=3.0 arc min. : manufacturing error; $\Delta\lambda$=3.0 arc min. ; $\Delta\alpha$=3.0 arc min

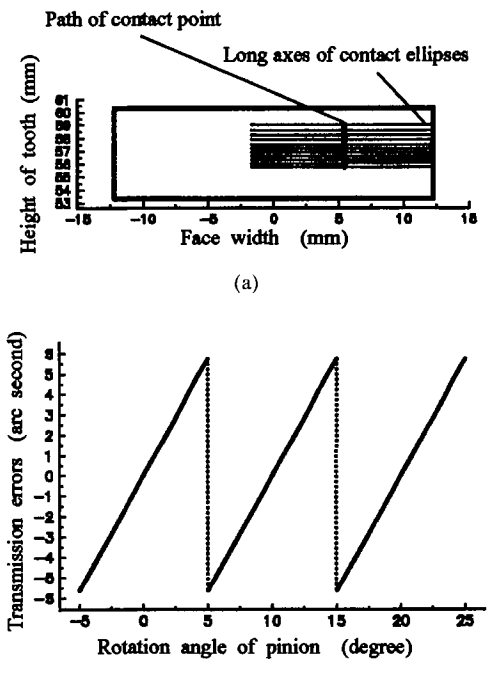

Fig. 6 (a) Bearing contact on pinion tooth surface (b) Corresponding transmission errors with lead crowning 0.02 mm of pinion; 0.0 mm of gear : misalignment; $\Delta E=0.1$ mm; $\Delta\gamma_y=3.0$ arc min. : manufacturing error; $\Delta\lambda=3.0$ arc min. ; $\Delta\alpha=3.0$ arc min

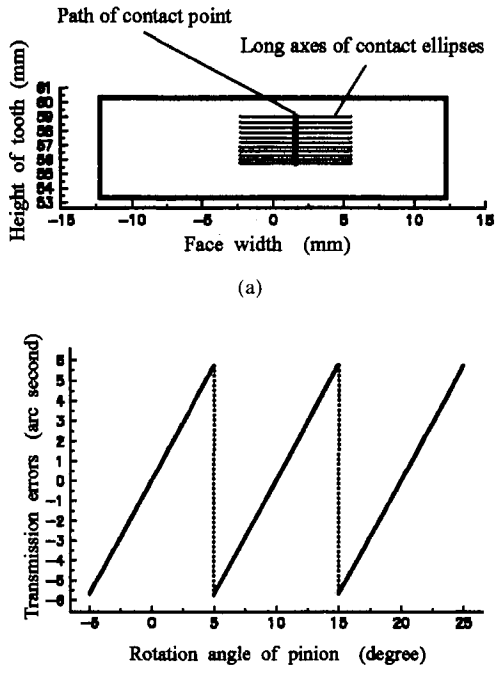

Fig. 7 (a) Bearing contact on pinion tooth surface (b) Corresponding transmission errors with lead crowning 0.03 mm of pinion; 0.03 mm of gear : misalignment; $\Delta E=0.1$ mm; $\Delta\gamma_y=3.0$ arc min. : manufacturing error; $\Delta\lambda=3.0$ arc min. ; $\Delta\alpha=3.0$ arc min

1800, 3600 rpm.

The results of computation are as follows.

(1) The application of crowning enables localization of the bearing contact (Figs. 5~7).

(2) The function of transmission errors of a crowned gear drive with geometric defects is a discontinuous one and the level is about 10 *arc seconds*, which may be a source of vibration and large dynamic force (Figs. 5~7).

(3) Although crowning of both members of drive is more expensive, it provides a more stable bearing contact than crowning done for only one drive member (Fig. 5 and Fig. 6). The same conditions of geometric defects have been considered for such comparison.

(4) Increased crowning can provide a more stable bearing contact; however due to smaller dimensions of contact ellipses the contact stress is increased and therefore the pitting durability is decreased (Figs. 5~7).

(5) If, in addition to lead crowning, the profile modification is applied with plunging operation during feeding of the grinding disk (Fig. 2(b)), the desirable type of transmission error can be achieved with stable bearing contact (Fig. 8(a), (b)).

(6) For the operating speed of 1800 rpm, the dynamic load is about 1.3 times that of the static load (Fig. 9(a)). For the operating speed of 900 rpm, the dynamic load is almost equivalent to the static load (Fig. 9(b)). This indicates that the dynamic effect of the geometric defects is minor in low speed operation (below 1000 rpm).

(7) For the operating speed of 3600 rpm, the geometric defects cause an increased dynamic load that is almost two times larger than that of the static load (Fig. 10(a)).

(8) If the predesigned parabolic function of the transmission errors is provided(Fig. 8(b)), the dymaic load is considerably reduced (Fig. 10

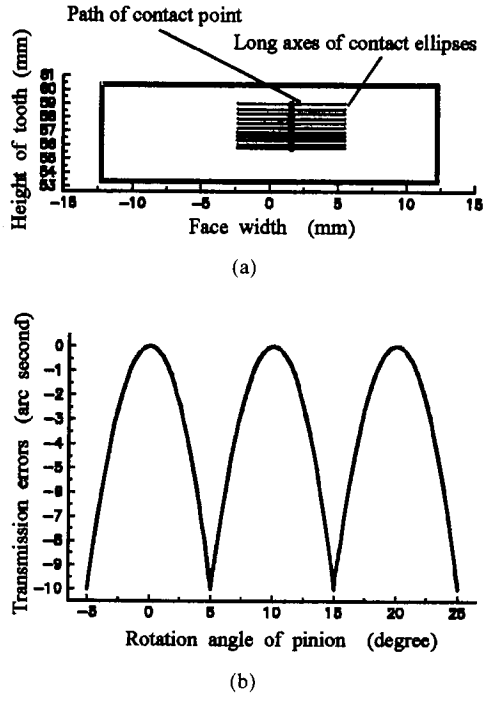

Fig. 8 (a) Bearing contact on pinion tooth surface (b) Corresponding transmission errors with lead crowning and profile modification: misalignment; $\Delta E=0.1$ mm; $\Delta\gamma_y=3.0$ arc min. : manufacturing error; $\Delta\lambda=3.0$ arc min. ; $\Delta\alpha=3.0$ arc min

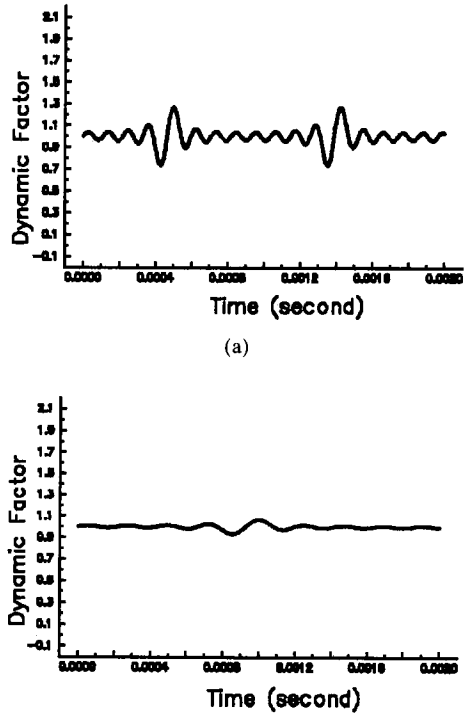

Fig. 9 Dynamic factor of crowned spur gear drive with (a) driving torque=160 Nm; operating velocity=1800 rpm (b) driving torque=160 Nm; operating velocity=900 rpm

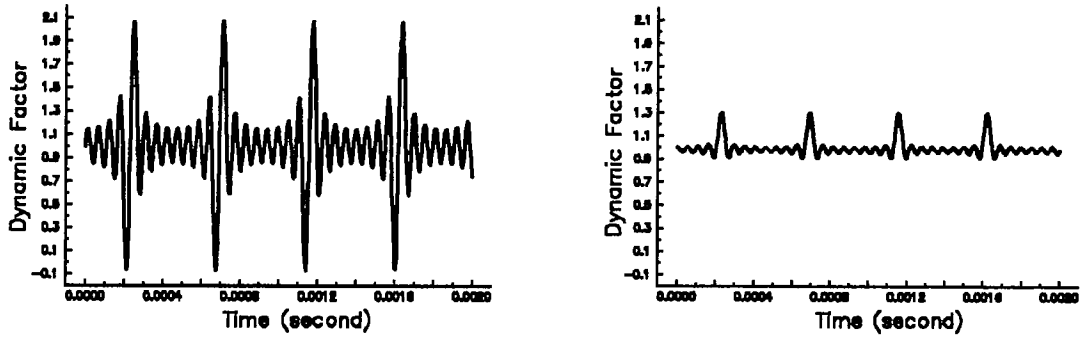

Fig. 10 Dynamic factor of (a) crowned spur gear drive and (b) crowned and profile modified spur gear drive with driving torque=160 Nm; operating velocity=3600 rpm

(b)). This was experimentally proved for spiral bevel gear drives in the previous research (Lewicki, 1993).

6. Conclusion

(1) A mathematical model for a crowned spur gear drive has been proposed and an approach has been developed to simulate meshing and

contact of the modified gear drive. The drive was considered as a multi-system of rigid body.

(2) The dynamic effect of transmission errors has been determined.

(3) Numerical computation was accomplished by the application of computer programs developed for tooth contact analysis and dynamic simulation.

(4) If complemented by experiments, the obtained results will enable one to design low-noise spur gear drives with extended service life.

References

AGMA, 1976, *Design Guide for Vehicle Spur and Helical Gears*, AGMA 170. 01.

Inhoy, Gu, 1997, "Design of Antibacklash Pin-gearing," *KSME International Journal*, Vol. 11, No. 6, pp. 611~619.

Kahraman, A. and Blankenship, G. W. 1997, "Experiments on Nonlinear Dynamic Behavior of an Oscillator with Clearance and Periodically Time-Varying Parameters," *ASME J. of Applie. Mechanics*, Vol. 64, pp. 217~226.

Lewicki, D. G., Handschuh, R. F., Zachary, S. H. and Litvin, F. L., 1993, "Low-Noise, High-Strength, Spiral-Bevel Gears for Helicopter Transmission," *NASA Technical Memorandum* 106080, AIAA-93-2149.

Lin, H-H., Huston, R. L. and Coy, J. J., 1988, "On Dynamic Loads in Parallel Shaft Transmissions: Part I -Modelling and Analysis," *ASME J. of Mechanical Design*, Vol. 110, pp. 221~225.

Litvin, F. L., 1989, *Theory of Gearing*, NASA.

Matsumura, S., Umezawa, K. and Houjoh, H., 1996, "Rotational Vibration of a Helical Gear Pair Having Tooth Surface Deviation during Transmission of Light Load," *JSME Series C*, Vol. 39, No. 3, pp. 614~620.

Savage, M., Brikmanis, C., Lewicki, D. G. and Coy, J. J., 1988, "Computerized Design, Life and Reliability Modeling of Bevel Gear Reductions," *ASME J. of Mechanical Design*, Vol. 110, pp. 189~196.

Seol, I. H. and Litvin, F. L., 1996, "Computerized Design, Generation and Simulation of Meshing and Contact of Modified Involute, Klingelnberg and Flender Type Worm-Gear Drives," *ASME J. of Mechanical Design*, Vol. 118, pp. 551~555.

Townsend, P.S. 1991, *Dudley's Gear Handbook*, 2nd ed. McGraw-Hill, NY.

Wang, C. C., 1985, "On Analytical Evaluation of Gear Dynamic Factors Based on Rigid Body Dynamics," *ASME J. of Mechanical Design*, Vol. 107, pp. 301~311.